

Quark-gluon vertex with an off-shell $O(a)$ -improved chiral fermion action

Huey-Wen Lin*

Physics Department, Columbia University, New York, NY 10027, USA

We perform a study the quark-gluon vertex function with a quenched Wilson gauge action and a variety of fermion actions. These include the domain wall fermion action (with exponentially accurate chiral symmetry) and the Wilson clover action both with the non-perturbatively improved clover coefficient as well as with a number of different values for this coefficient. We find that the domain wall vertex function behaves very well in the large momentum transfer region. The *off-shell* vertex function for the *on-shell* improved clover class of actions does not behave as well as the domain wall case and, surprisingly, shows only a weak dependence on the clover coefficient c_{SW} for all components of its Dirac decomposition and across all momenta. Including off-shell improvement rotations for the clover fields can make this action yield results consistent with those from the domain wall approach, as well as helping to determine the off-shell improved coefficient c'_q .

PACS numbers: 11.15.Ha, 11.30.Rd, 12.38.Gc, 12.38.Lg, 14.70.Dj

I. INTRODUCTION

The study of gauge-fixed quark and gluon correlation functions on the lattice is a useful tool to understand the non-perturbative behavior of QCD. Within lattice QCD one may hope that the quark-gluon vertex in particular may be a momentum dependent probe that displays discretization effects beyond those seen in the free field case. Indeed one may hope that knowledge of the quark-gluon vertex allows the determination of improvement coefficients without resort to Ward identities. This may allow the non-perturbative $O(a)$ improvement obtained in the light quark limit for clover fermions[1] using the PCAC relation to be extended to the Fermilab action[2] at arbitrary quark mass.

Beyond lattice QCD knowledge of the non-perturbative n -point functions gives the only theoretical access to the deeply infra-red sector of the theory and may be used to provide non-perturbative information for model calculations. Further we can obtain the non-perturbative running of a physically defined coupling, and may be able to use these non-perturbative correlation functions in the Dyson-Schwinger equations. DSEs are of qualitative and quantitative importance in understanding dynamical chiral symmetry breaking and confinement, and simulations of lattice QCD also provide access to QCD's Schwinger functions. Previous studies of the quenched theory have yielded gluon[3] and clover quark[4] propagators and the quark-gluon vertex on the lattice has also been studied extensively[5]. These previous studies of the vertex were limited to the on-shell improved, non-chirally symmetric clover action, and post-simulation field rotations were used to implement off-shell improvement.

The domain wall chiral fermion action[6] is automatically $O(a)$ -improved, and domain wall fields should greatly aid studies of off-shell correlation functions. The off-shell quark propagator has been previously and comprehensively studied for the domain wall fermion action[7], and renormalization constants were determined for many fermion bilinears in the chiral limit for the Wilson and DBW2 gauge actions. The off-shell properties of the propagator were found to be remarkably continuum-like for this action, and one expects that this would also be seen for the domain wall vertex function.

In this paper we also use this more advanced domain wall fermion action, which is chirally symmetric (bar exponentially small terms), and demonstrate that such improvement is indeed seen in our calculations of the quark-quark-gluon three-point function and the vertex function.

Further, one might expect that a Dirac structure decomposition of the vertex function could be used to match the clover action (with field rotations) to the domain wall action. This could provide a mechanism for fixing the clover coefficient non-perturbatively without the imposition of the PCAC relation, and it was hoped that this would allow a non-perturbative clover coefficient determination for all quark masses[8]. However we find weak dependence on this coefficient after absorbing a trivial mass renormalization and instead find the correlation function is most sensitive to the c'_q improvement parameter.

The structure of this paper is as follows: Section II defines the notation and lattice correlation functions measured to obtain gauge-fixed two-point and three-point functions. Section III lists details of the simulation parameters. Section IV presents the gauge-fixing strategy used. Sections V and VI present simulation results of the quark and gluon two-point functions. Section VII presents simulation results of the quark-quark-gluon three-point function and the truncated vertex. Section VIII discusses the off-shell improvement and contrasts the DWF and clover cases. Finally, Section IX presents

*Electronic address: hwlin@theory1.phys.columbia.edu

a summary, conclusions, and future outlook for this program.

II. NON-PERTURBATIVE GREEN FUNCTIONS: DEFINITION

A. Off-shell $O(a)$ improvement

The on-shell $O(a)$ -improved Wilson clover action[9] can be written as

$$S = a^4 \sum_{x,x'} \bar{\psi}(x) (D_c + m)_{xx'} \psi(x') \quad (1)$$

$$\begin{aligned} (D_c + m)_{xx'} &= m - \frac{1}{2a} \sum_{\mu} \left\{ (1 - \gamma_{\mu}) U_{x,\mu} \delta_{x+\hat{\mu},x'} \right. \\ &\quad \left. + (1 + \gamma_{\mu}) U_{x',\mu}^{\dagger} \delta_{x-\hat{\mu},x'} \right\} \\ &\quad + \left\{ \frac{4}{a} + \frac{ic_{\text{SW}}}{4} \sum_{\mu,\nu} \sigma_{\mu\nu} F_{\mu\nu,xx'} \right\} \delta_{x,x'} \quad (2) \\ F_{\mu\nu,xx'} &= \frac{1}{2a^2} \left\{ U_{x,\mu} U_{x+\hat{\mu},\nu} U_{x+\hat{\nu},\mu}^{\dagger} U_{\nu}^{\dagger} \right. \\ &\quad - U_{x-\hat{\nu},\nu}^{\dagger} U_{x-\hat{\nu}-\hat{\mu},\mu}^{\dagger} U_{x-\hat{\nu}-\hat{\mu},\nu} U_{x,\mu} \\ &\quad + U_{x,\nu} U_{x+\hat{\nu}-\hat{\mu},\mu}^{\dagger} U_{x-\hat{\mu},\nu}^{\dagger} U_{x-\hat{\mu},\mu} \\ &\quad \left. - U_{x,\mu} U_{x-\hat{\nu}+\hat{\mu},\nu}^{\dagger} U_{x-\hat{\nu},\mu}^{\dagger} U_{x-\hat{\nu},\nu} \right\}. \quad (3) \end{aligned}$$

To *off-shell* improve the physical quantities calculated from this Wilson clover action, we keep the action unchanged but perform post-simulation rotations[10] to improved quark fields of the form

$$\begin{aligned} \psi &\rightarrow \hat{\psi} = Z_q^{\frac{1}{2}} [1 + ac'_q (D_c + m) + ac_{\text{NGI}} \gamma_{\mu} \partial_{\mu}] \psi \\ \bar{\psi} &\rightarrow \hat{\bar{\psi}} = Z_q^{\frac{1}{2}} \bar{\psi} \left[1 + ac'_q (-\overleftarrow{D}_c + m) - ac_{\text{NGI}} \gamma_{\mu} \overleftarrow{\partial}_{\mu} \right] \quad (4) \end{aligned}$$

The improved quark propagator $S_I(x) \equiv \langle \hat{\psi}(x) \hat{\bar{\psi}}(0) \rangle$ can then be expressed in terms of the unimproved quark propagator. In momentum space, we have:

$$\begin{aligned} S_I(p) &= Z_q \left[(S_L(p) + 2ac'_q) \right. \\ &\quad \left. + ac_{\text{NGI}} \left\{ i\gamma_{\mu} \frac{pa}{a}, S_L(p) \right\} \right] + O(a^2) \quad (5) \end{aligned}$$

where S_L is the unimproved quark propagator. The constant c_{NGI} has been previously demonstrated to be zero at tree level[10] and small for light quark masses[11].

The domain wall fermion (DWF) action[6] is

$$D_{x,s;x',s'} = \delta_{s,s'} D_{x,x'}^{\parallel} + \delta_{x,x'} D_{s,s'}^{\perp} \quad (6)$$

$$\begin{aligned} D_{x,x'}^{\parallel} &= \frac{1}{2} \sum_{\mu=1}^4 \left[(1 - \gamma_{\mu}) U_{x,\mu} \delta_{x+\hat{\mu},x'} + (1 + \gamma_{\mu}) U_{x',\mu}^{\dagger} \delta_{x-\hat{\mu},x'} \right] \\ &\quad + (M_5 - 4) \delta_{x,x'} \quad (7) \end{aligned}$$

$$\begin{aligned} D_{s,s'}^{\perp} &= \frac{1}{2} \left[(1 - \gamma_5) \delta_{s+1,s'} + (1 + \gamma_5) \delta_{s-1,s'} - 2\delta_{s,s'} \right] \\ &\quad - \frac{m_f}{2} \left[(1 - \gamma_5) \delta_{s,L_s-1} \delta_{0,s'} + (1 + \gamma_5) \delta_{s,0} \delta_{L_s-1,s'} \right], \quad (8) \end{aligned}$$

where s and s' lie in the range $0 \leq s, s' \leq L_s - 1$, M_5 is the five-dimensional mass, and m_f directly couples the two domain walls at $s = 0$ and $s = L_s - 1$. The DWF action is $O(a)$ off-shell improved due to its exponentially accurate chiral symmetry[7], and no further improvement in the action or quark fields is performed.

B. The gluon field

The lattice gluon field A_{μ}^a is defined by

$$\begin{aligned} A_{\mu}^a(x + \hat{\mu}/2) \tau^a &= \frac{1}{2ig_0} \left[(U_{\mu}(x) - U_{\mu}^{\dagger}(x)) \right. \\ &\quad \left. - \frac{1}{3} \text{Tr} (U_{\mu}(x) - U_{\mu}^{\dagger}(x)) \right] + O(a^3), \quad (9) \end{aligned}$$

where a is the color index, μ is the Lorentz index, g_0 is the bare coupling constant, and $\text{Tr}\{\tau^a \tau^b\} = \frac{1}{2} \delta_{ab}$.

The gluon propagator (in Landau gauge) is

$$D_{\mu\nu}^{ab}(q) = \frac{1}{V} \langle A_{\mu}^a(q) A_{\nu}^b(-q) \rangle \simeq \delta_{ab} P_{\mu\nu} D(q^2), \quad (10)$$

where $D(q^2) = \frac{1}{24} \sum_{\mu,a} D_{\mu\mu}^{aa}(q)$ and $P_{\mu\nu} = \delta_{\mu\nu} - \frac{q_{\mu} q_{\nu}}{q^2}$.

C. The quark-gluon vertex function

The quark-gluon vertex function can be calculated from the following three-point function[5]:

$$V_{\mu}^a(x, y, z)_{\alpha\beta}^{ij} = \langle S_{\alpha\beta}^{ij}(x, z) A_{\mu}^a(y) \rangle. \quad (11)$$

where the lattice gluon field A_{μ}^a is defined in Eq. 9. The Fourier-transformed, amputated and transverse-projected vertex function in momentum space for Landau gauge is given by

$$\begin{aligned} \Lambda_{\mu}^{P,a,\text{lat}}(p, q)_{\alpha\beta}^{ij} &= \Lambda_{\mu}(p, q)_{\alpha\beta}^{ij} \tau_{ij}^a = P_{\mu\nu} \Lambda_{\nu}^{a,\text{lat}}(p, q)_{\alpha\beta}^{ij} \\ &= \langle S(p) \rangle^{-1} P_{\mu\nu} V_{\nu}^a(p, q)_{\alpha\beta}^{ij} \langle S(p+q) \rangle^{-1} \langle D(q) \rangle^{-1} \quad (12) \end{aligned}$$

where the projected vertex function is introduced since the gluon propagator is singular for general momenta, posing problems for a full amputation. Note that the S means $S_L(p)$ for the bare vertex and $S_I(p)$ for the off-shell improved clover quark field.

In the case of $q = 0$ the gluon propagator is no longer proportional to the projection $P_{\mu\nu}$, but rather is

$$\begin{aligned} \Lambda_{\mu}^{a,\text{lat}}(p, q=0)_{\alpha\beta}^{ij} &= \langle S(p) \rangle^{-1} P_{\mu\nu} V_{\nu}^a(p, q=0)_{\alpha\beta}^{ij} \langle S(p) \rangle^{-1} \langle D(0) \rangle^{-1} \quad (13) \end{aligned}$$

The non-perturbative gluon propagator in a finite volume remains well defined and the same amputation process is used.

III. SIMULATION PARAMETERS

All of the calculations in this paper were performed with the Wilson gauge action[12] in the quenched approximation at $\beta = 6.0$, $a^{-1} = 1.922(40)$ GeV with a $16^3 \times 32$ lattice size[13]. The simulation was performed using a heatbath algorithm with 2000 thermalization sweeps and 500 measurements, separated by 2000 sweeps each.

The fermion actions used are DWF and the Wilson clover action with various parameters. The details are listed in Table I, and we note that the pseudoscalar masses for three of the clover action combinations were (somewhat approximately) matched to the domain wall pseudoscalar mass using a single, low-statistics pass.

TABLE I: Simulation parameters

Label	Parameters	PS meson
DWF	$M_5 = 1.8$, $L_s = 16$, $ma = 0.0125$	442(9) MeV
$c_{\text{SW}} = 1.769$	$\kappa = 0.1346$, $c_{\text{SW}} = 1.769$	470(10) MeV
$c_{\text{SW}} = 1.5$	$\kappa = 0.1382$, $c_{\text{SW}} = 1.5$	462(11) MeV
$c_{\text{SW}} = 2.0$	$\kappa = 0.1313$, $c_{\text{SW}} = 2.0$	452(13) MeV
$c_{\text{SW}} = 1.479$	$\kappa = 0.1370$, $c_{\text{SW}} = 1.479$	796(8) MeV

We use periodic boundary conditions for both the spatial and temporal directions to calculate both the fermionic and gluonic propagators. The momenta used for Fourier transformation are $p_\mu = 2\pi n_\mu/L_\mu$, with $|n_{\{x,y,z\}}| \in \{0, 1, 2\}$ and $|n_t| \in \{1, 2\}$.

IV. GAUGE FIXING STRATEGY

Since we are interested in gauge-dependent off-shell quantities we choose to fix to a convenient gauge, namely Landau gauge, by maximizing the following functional:

$$F[U_\mu(n), g(n)] = 1 - \sum_{\mu, n} \text{ReTr} U_\mu^g(n), \quad (14)$$

where $U_\mu^g(n) = g(n)U_\mu(n)g(n + \hat{\mu})^\dagger$ with gauge transformation matrix $g(n)$. The gauge-fixing stopping condition is

$$\frac{1}{N_c V} \sum_n \text{Tr} (B(n)B(n)^\dagger) \leq 10^{-8} \quad (15)$$

where N is the number of total sites on the lattice and

$$B(n) = C(n) - C(n)^\dagger - \frac{1}{3} \text{Tr} (C(n) - C(n)^\dagger), \quad (16)$$

$$C(n) = \left(U_\mu^g(n)^\dagger + U_\mu^g(n - \hat{\mu}^\dagger) \right). \quad (17)$$

Landau gauge suffers from Gribov ambiguities[14], and due care must be taken to ensure our results are not significantly affected. We checked for the influence of Gribov copies on each of our observables by gauge fixing in

two ways. The first is naively fixing to Landau gauge in the usual way, and the second involves fixing to Landau gauge from a deterministic starting gauge orbit, by first fixing to maximal axial gauge[15]. This is a common approach which gives a deterministic Gribov copy, independent of the gauge of the initial lattice configuration.

We found that the two different procedures agree for the gluon propagator, have slight effects on quark propagators (decreasing as the momentum increases) but give very different results in the vertex calculation[8], as shown in Figure 1. We believe the differences are caused by Gribov copies and from now on, we will follow the deterministic procedure for better control over this effect.

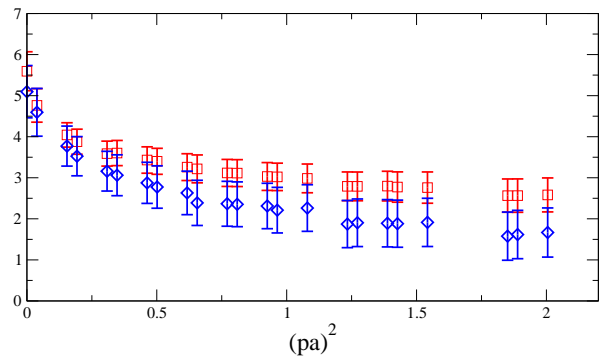


FIG. 1: Comparison between Landau gauge fixing with (squares) and without (diamonds) first fixing to maximal axial gauge for the vertex function.

V. FERMIONIC TWO-POINT GREEN FUNCTION

We start from the two-point function used for non-perturbative renormalization in the RI-MOM scheme[16]. The quark and gluon propagators from quenched lattice configurations have been well studied previously for both fermion actions[4, 7]. However, these remain a prerequisite for our exploratory study of the vertex function, and our results must be defined and introduced prior to moving on to the vertex function.

The bare quark field renormalization factor, $Z_q(p^2)$, is calculated from

$$Z_q(pa) = \frac{-i}{12 \sum_\mu (p_\mu a)^2} \text{Tr} \left(\sum_\mu p_\mu a \gamma_\mu S_L^{-1} \right), \quad (18)$$

where, as we shall see, constraints on the above quantity in the matching window allow Z_q to be determined from a fit.

In Figure 2 we show the bare quark field renormalization $Z_q((pa)^2)$ for each of the actions listed in Table I using the bare fields. We calculate the Z_q factor in the RI-MOM scheme by removing the expected perturbative

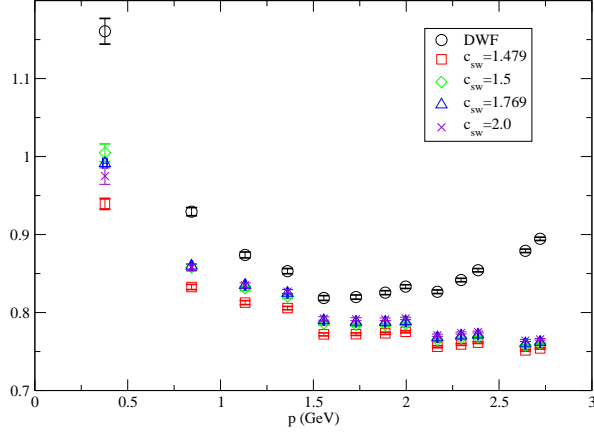


FIG. 2: The quark field renormalization factor Z_q for different actions.

momentum dependence to define a scale invariant quantity Z_q^{SI} ,

$$Z_q^{\text{SI}}((pa)^2) = Z_q((pa)^2)/C_A((pa)^2), \quad (19)$$

and then fit the $(pa)^2$ dependence of this SI expression to the form $f_1 + f_2(pa)^2$ where the f_2 term absorbs lattice artifacts.

From this we obtain the phenomenologically relevant renormalization factor between the lattice and the $\overline{\text{MS}}$ scheme.

$$\frac{Z^{\text{RI}}}{Z^{\overline{\text{MS}}}} = 1 + \frac{\alpha_s}{4\pi} Z_0^{(1)\text{RI}} + \frac{\alpha_s^2}{(4\pi)^2} Z_0^{(2)\text{RI}} \quad (20)$$

where definition and values for $C_A((pa)^2)$, α_s , $Z_0^{(1)\text{RI}}$ and $Z_0^{(2)\text{RI}}$ are well known[7]. Figure 3 shows Z_q for these three schemes for domain wall fermions.

Table II shows our results for the various fermion actions under consideration. As one would expect, where previous data exists for the same action, these results are consistent. In particular, for the domain wall action we refer the reader to Ref. [7] where the massless limit was taken.

TABLE II: Quark field renormalization factor for the fitting range of $0.8 \leq (pa)^2 \leq 2.0$.

Label	Z^{SI}	$Z^{\overline{\text{MS}}}$
DWF	0.802(9)	0.806(9)
$c_{\text{sw}} = 1.479$	0.825(6)	0.829(6)
$c_{\text{sw}} = 1.5$	0.840(6)	0.844(6)
$c_{\text{sw}} = 1.769$	0.846(6)	0.850(6)
$c_{\text{sw}} = 2.0$	0.849(6)	0.854(6)

Following Ref. [10], we expect that in the large momentum region the scalar part of the quark propagator

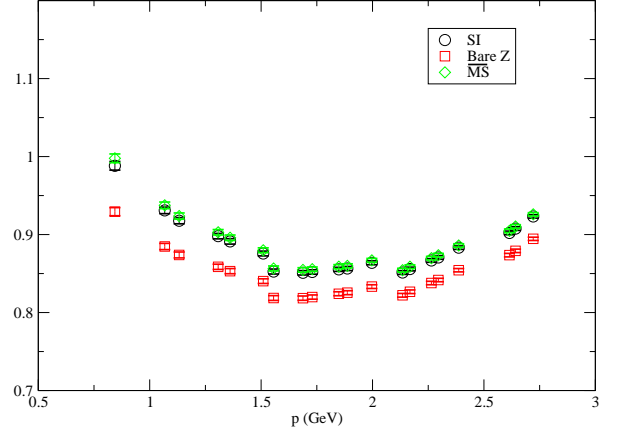


FIG. 3: The quark field renormalization factor Z_q for the bare, SI and $\overline{\text{MS}}$ schemes on our DWF data set.

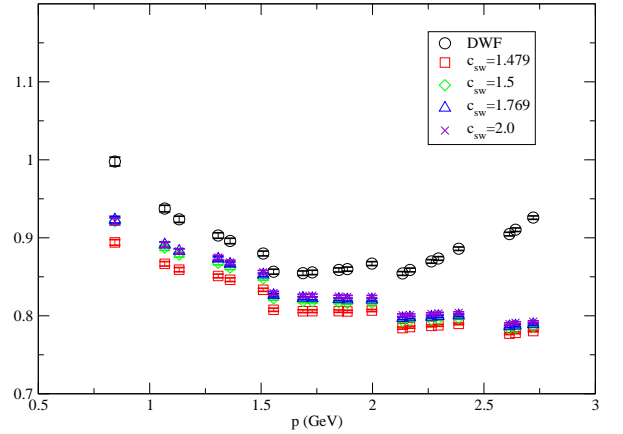


FIG. 4: The quark field renormalization factor $Z_q^{\overline{\text{MS}}}((pa)^2)$ for different actions.

behaves like

$$\frac{1}{12} \text{Tr}(S_L(p)) = C \times (pa)^2 + (-2c'_q + 2c_{\text{NGI}}Z_q) + \frac{Z_q Z_m m_I}{p^2} + O\left(\frac{1}{p^4}\right). \quad (21)$$

As mentioned in Subsection II A, c_{NGI} is zero at tree level and has been found to be numerically very small in the light quark region[11], enabling us to take it as zero in our calculation. Therefore, we can use this formula to determine c'_q .

The resulting parameters, used later in this paper, are displayed in Table III. We note that the first two terms in Eq. 21 violate chiral symmetry and are not allowed in the DWF case. Our values for the clover actions are plausible given tree-level estimates of around 0.25.

TABLE III: Fitting to the first three terms in Eq. (21) with fitting range of $0.8 \leq (pa)^2 \leq 2.0$ produces the improvement coefficient c'_q .

Label	c'_q
$c_{\text{sw}} = 1.479$	-0.247(19)
$c_{\text{sw}} = 1.5$	-0.258(19)
$c_{\text{sw}} = 1.769$	-0.257(19)
$c_{\text{sw}} = 2.0$	-0.252(19)

VI. GLUONIC TWO-POINT GREEN FUNCTION

There are many renormalization schemes that may be applied to the gluon propagator, and one of the more common in the literature is the MOM scheme where the gluon field renormalization factor is constrained by requiring that, at some fixed scale μ , an effective tree level Coulombic form holds:

$$Z_3^{\text{RI}}(\mu)D(q^2; \mu)|_{q^2=\mu^2} = \frac{1}{\mu^2}. \quad (22)$$

The quantity $Z_3(q^2)^{-1} = q^2 D(q^2)$ is displayed in Figure 5, and we see that this condition leads to a renormalization constant Z_3 that is highly sensitive to the scale μ in the momentum regions currently accessible to lattice QCD.

This scale dependence is an artifact of the renormalization condition, and we pick a fixed renormalization point $a\mu = 1$ and use the one-loop form[17] of the running to present the data in a manner that should be perturbatively scale-invariant:

$$(Z_3^{\text{SI}}(q^2))^{-1} = q^2 D(q^2) \left[\frac{\log(\frac{q^2}{\Lambda^2})}{\log(\frac{\mu^2}{\Lambda^2})} \right]^{d_D}, \quad (23)$$

where $d_D = \frac{13}{22}$ for the quenched approximation in Landau gauge, $a\mu = 1$ by choice, and $\Lambda = 0.35(5)$ is obtained from a fit to the propagator. We note that the error is obtained from the sensitivity of the result to the upper limit of this fit range in the region $0.5 \leq (aq)^2 \leq 2.0$. Our value for Λa is identical to that obtained in Ref. [18] when fitted over the range used in that paper, but it shows great sensitivity to the range.

We can see that this scale invariant presentation in Figure 6 shows a nice plateau demonstrating perturbative behavior and gives confidence in our result at and around this renormalization point. We obtain the MOM scheme renormalization constant as $(Z_3^{\text{SI}})^{-1} = 2.45(1)$ at the scale of $\mu = a^{-1} = 1.922(40)$ GeV.

A more conventional approach would be to use the $\overline{\text{MS}}$ scheme at some scale. However, the conversion to this scheme is not known and we isolate this lack of knowledge, localizing it to a single continuum renormalization constant $\overline{Z}_3(\overline{\mu})$ which converts from the RI-MOM scheme at $a\mu = 1$ to the $\overline{\text{MS}}$ scheme at momentum scale $\overline{\mu}$.

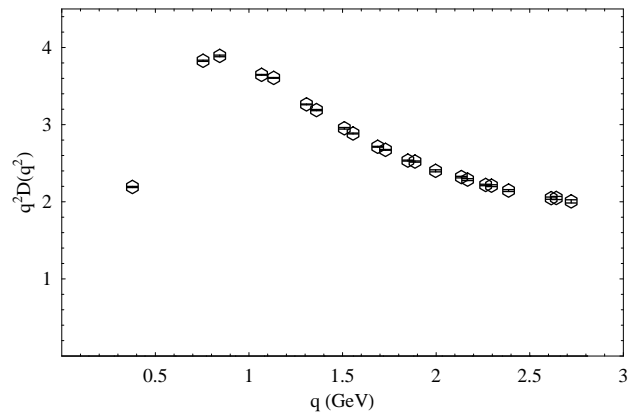


FIG. 5: The naïve RI-MOM scheme renormalization constant $Z_3^{-1} = q^2 D(q^2)$ in Landau gauge.

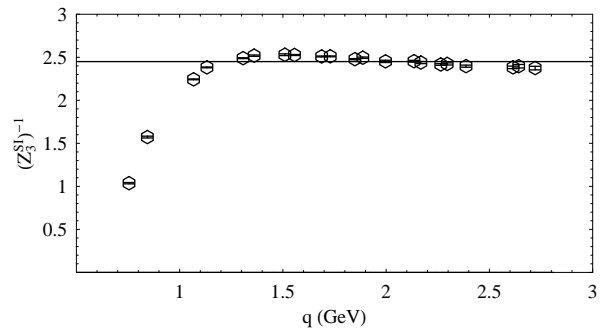


FIG. 6: Scale invariant MOM scheme renormalization constant $Z_3^{\text{SI}}(q^2)^{-1}$ at fixed renormalization point $(a\mu)^2 = 1$.

VII. QUARK-QUARK-GLUON THREE-POINT FUNCTION

We consider the three-point function consisting of a gluon with incoming momentum q and two quarks with incoming momentum p and $-(p+q)$ as shown in Figure 7.

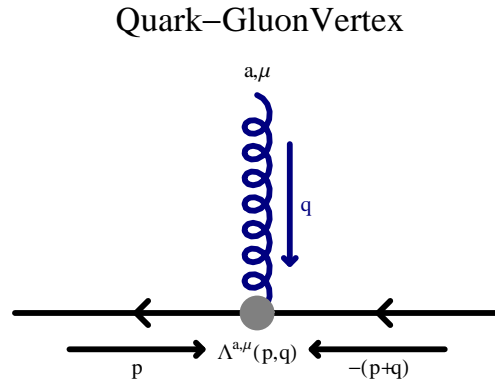


FIG. 7: Quark-quark-gluon momentum space, three-point function.

A. Lorentz structure of vertex

In the continuum the vertex function has been expressed in terms of its general Lorentz structure in Ref. [5]. This decomposition is complex and requires a comprehensive set of lattice momenta to resolve the different components.

In the following subsections we will study kinematic regions that simplify the form factors appearing in the decomposition allowed by Lorentz symmetry in each case. As usual, appropriate spin and momentum projections can be used to determine the form factors from the bare lattice data.

B. Hard recoil kinematics

We first require both quark lines to carry momentum p giving a gluon momentum of $-2p$. In this case the vertex function may be decomposed as follows

$$\Lambda_\mu^P(p, q = -2p) = -ig [\lambda'_1(q^2) (\gamma_\mu - \not{q} q_\mu / q^2) - i\tau_5(q^2) \sigma_{\mu\nu} q_\nu]. \quad (24)$$

The form factors λ'_1 and τ_5 can be easily separated by different Lorentz projections.

C. Soft gluon kinematics

Next we choose the point $q = 0$. At this kinematic point the tensor contribution vanishes, and we may write these form factors in terms of their popular Lorentz decomposition as follows:

$$\Lambda_\mu(p, q = 0) = -ig [\lambda_1(p^2) \gamma_\mu - 4\lambda_2(p^2) \not{p} p_\mu - 2i\lambda_3(p^2) p_\mu]. \quad (25)$$

The form factors λ_1 and λ_2 are coupled by the same Lorentz projections but can be decoupled as following:

$$\lambda_1(p^2) = \frac{1}{36} \sum_\mu \text{Tr} \left(\gamma_\mu \sum_\nu \left(\delta_{\mu,\nu} - \frac{p_\mu p_\nu}{p^2} \right) \Lambda_\nu^{\text{lat}} \right) \quad (26)$$

$$\lambda_2(p^2) = \frac{1}{48(pa)^2} \left[\sum_\mu \text{Tr} (\gamma_\mu \Lambda_\mu^{\text{lat}}) - \frac{4}{3} \lambda_1(p^2) \right] \quad (27)$$

$$\lambda_3(p^2) = \frac{i}{24(pa)^2} \sum_\mu \text{Tr} (p_\mu \Lambda_\mu^{\text{lat}}). \quad (28)$$

Our method projects λ_1 and λ_2 for general kinematics while in Ref. [5] the authors use only kinematic points with $p_\mu = 0$ to isolate λ_1 from λ_2 .

D. Tree-level lattice perturbation theory

Here we note that the tree-level vertex function for the clover lattice action (without off-shell improvements) is

$$\Lambda_\mu^{[0],\text{lat}} = \gamma_\mu \cos \left(p_\mu a + \frac{1}{2} q_\mu a \right) - i \sin \left(p_\mu a + \frac{1}{2} q_\mu a \right) + \frac{1}{2} c_{\text{SW}} \cos \left(\frac{1}{2} q_\mu a \right) \sum_{\mu \neq \nu} \sigma_{\mu\nu} \sin(q_\nu a). \quad (29)$$

Thus, we might expect that to leading-order the clover action will be most sensitive to the clover coefficient through terms proportional to $\sigma_{\mu\nu}$. Therefore, in investigating the feasibility of fixing the clover coefficient from the vertex function we will consider the vertex function defined from bare (un-rotated) quark fields. We shall see later that, somewhat interestingly, this turned up a negative result.

Note that in subsection VII E, we will use the “bare” clover action to calculate the various form factors to avoid contamination from the poor choice of off-shell improved coefficients, while in subsection VII F, we will focus on the off-shell improved vertex with the non-perturbatively improved clover action.

E. Form factors

Figures 8-12 display the lattice results for $\lambda_1(p^2)$, $\lambda_2(p^2)$, $\lambda_3(p^2)$, $\lambda'_1(p^2)$, and $\tau_5(p^2)$ in the $\overline{\text{MS}}$ scheme using the renormalization constants calculated earlier in this paper, up to the unknown constant $\overline{Z}_3(\overline{\mu})$ in Section VI. This is shown for both the bare clover actions and the domain wall action. We will discuss the off-shell improvement of the clover action via post-simulation rotations in the following section.

We note that the off-shell improved DWF action in general shows a marked difference in the λ_3 scalar form-factor; see Figure 11, in particular. The difference between the DWF and clover action results is likely to be caused by the off-shell improvement present with domain wall fermions, and one might hope that the form factor λ_3 would be a good means to adjust the off-shell improvement coefficients for clover actions. There will be more discussion in Section VII F on this possibility.

The quantity λ'_1 is the form factor reflecting the γ^μ term in the fermion action. This quantity appears to be the most similar among the actions studied here.

As seen in Figure 12, we find no statistically significant evidence of c_{SW} dependence in the σ projection of the vertex function, despite both its leading order contribution to the tree-level vertex and our examining it at a sizeable range of lattice momenta.

The difference between the (bare) clover and DWF actions is again quite marked and may be in principle useful for determining off-shell improvement rotations. However, since c_{SW} (in perturbation theory) couples with this

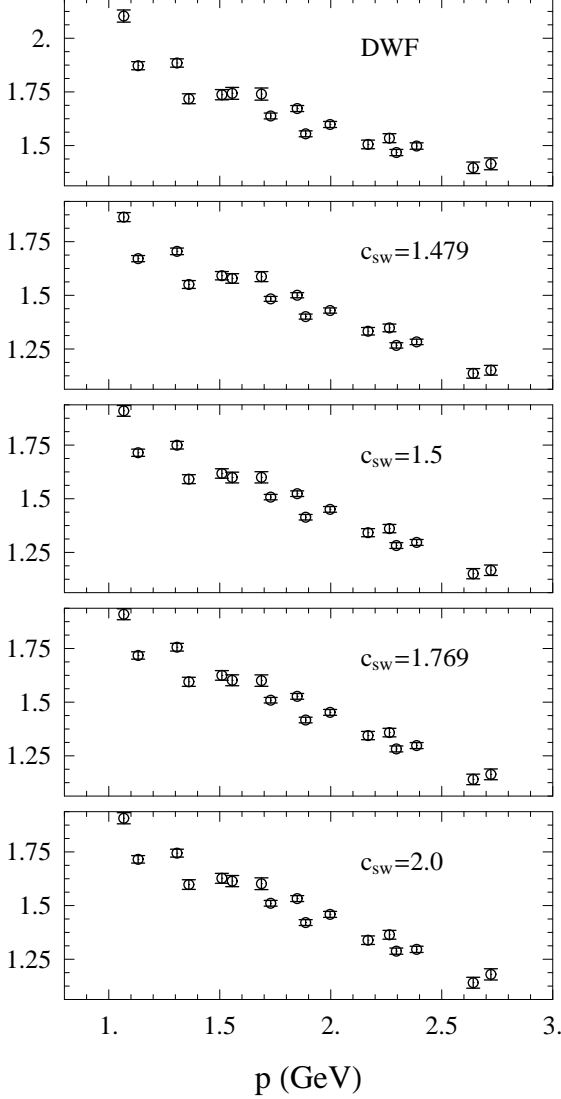


FIG. 8: The vector vertex function form factor $\lambda_1(p^2)/\overline{Z}_3(\overline{p})$ for the soft gluon case. This is displayed for both the chirally symmetric DWF action and the bare clover action.

vertex function at leading order and since the non-zero gluon momenta are statistically noisier, we will only calculate the c'_q from λ_3 .

F. Determining c'_q directly from the vertex function

The quantity c'_q appearing in the improved quark field can be calculated from the quark propagator alone, as demonstrated previously in Refs. [10, 11] and in this work. Here we propose and will demonstrate that we can determine this coefficient independently by matching form factors to the already improved DWF vertex function for the $q = 0$ kinematics. Any consistency between these two independent determinations of c'_q will contribute to the body of evidence that c_{NGI} is near zero.

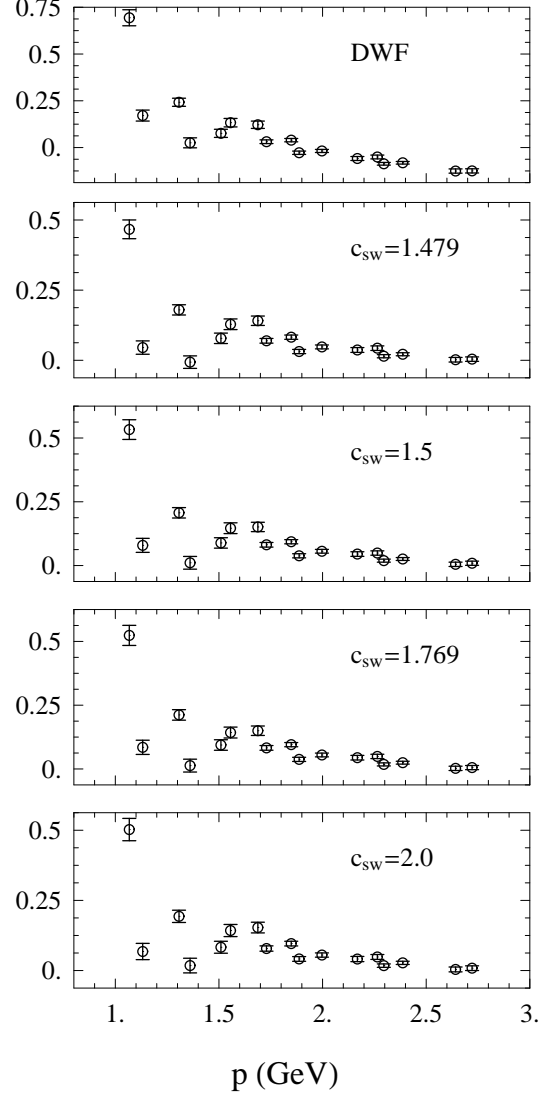


FIG. 9: The vector vertex function form factor $\lambda_2(p^2)/\overline{Z}_3(\overline{p})$ for the soft gluon case. This is displayed for both the chirally symmetric DWF action and the bare clover action.

1. Tree-level calculation

If we apply the off-shell quark field improvement of Eq.(4), we obtain the following expression for the tree-level vertex function[8]:

$$\begin{aligned}
 \Lambda_\mu^{[0]} = & \{i \sin(p_\mu a + q_\mu a/2)(-1 + 2c_q) \\
 & + ic_{\text{NGI}} [\sin(p_\mu a + q_\mu a) + \sin(p_\mu a)] \cos(p_\mu a + q_\mu a/2)\} \\
 & - \gamma_\mu \{\cos(p_\mu a + q_\mu a/2)(1 + 4c_q m a)\} \\
 & + i\sigma_{\mu\nu} \{i/2 \cos(q_\mu a/2) \sin(q_\nu a)(c_{\text{sw}} - 2c_q) \\
 & + ic_{\text{NGI}} [\sin(p_\nu a + q_\nu a) - \sin(p_\nu a)] \cos(p_\mu a + q_\mu a/2)\}
 \end{aligned} \tag{30}$$

which depends on the coefficients of c'_q ($= -0.5c_q$) and c_{NGI} . As above we assume c_{NGI} is zero, so the only task

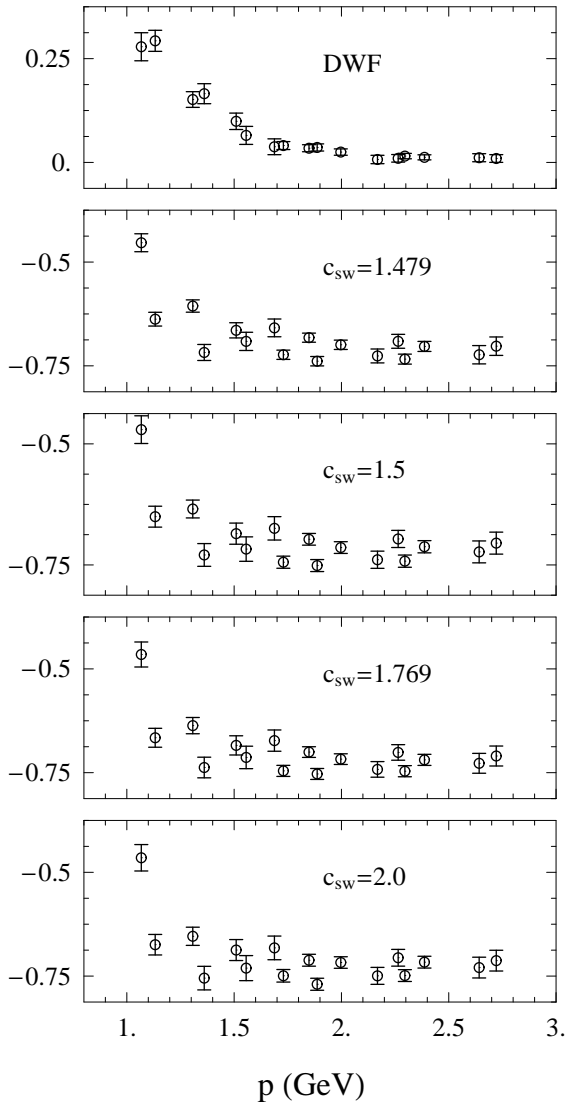


FIG. 10: The scalar vertex function form factor $\lambda_3(p^2)/\overline{Z}_3(\overline{p})$ for the soft gluon case. This is displayed for both the chirally symmetric DWF action and the bare clover action.

is to determine the quantity c'_q from the vertex function.

This expression illuminates how the different form factors might be expected to depend (to leading order) on the different improvement coefficients. In particular, we note the leading-order sensitivity of the $\sigma_{\mu\nu}$ piece, τ_5 , to the clover coefficient.

2. Numerical work

Here we consider the clover action with the non-perturbative c_{sw} coefficient. We included the ma dependence (from on-shell improvement) by replacing the Z_q in Eq.(4) with $(1 + b_q ma)Z_q$ for the clover action and performed the same calculation steps as in the unimproved field cases. Since the ma is small and b_q is 1.0

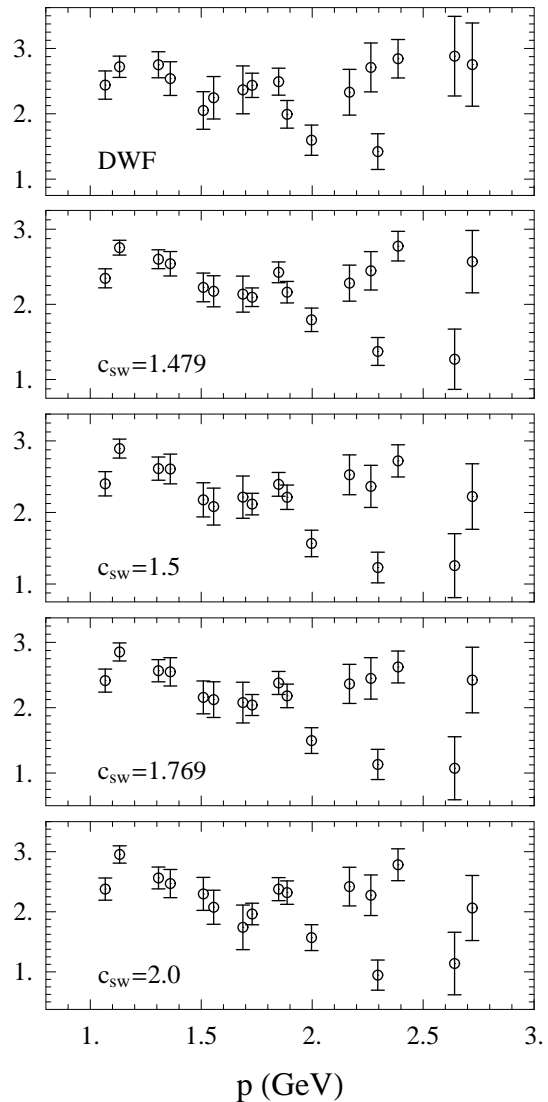


FIG. 11: The vector vertex function form factor $\lambda'_1(p^2)/\overline{Z}_3(\overline{p})$ for the hard-recoil kinematics. This is displayed for both the chirally symmetric DWF action and the bare clover action.

at tree level, we expected the contribution from b_q to be negligible. Indeed, we saw no significant changes in the calculation on quark propagator and form factors from quark-gluon vertex function.

In Figure 13 we compare the three form factors λ_1 , λ_2 and λ_3 between the domain wall and bare clover actions where the latter are computed for various values of $c'_q \in \{0.0, -0.20, -0.257\}$ and with b_q taking its tree-level value, $b_q = 1.0$. As we predict from our tree-level exercises, the form factor λ_3 is indeed very sensitive to c'_q . The calculation shows that our value for c'_q calculated from quark propagator is closest to the DWF result, although at large momentum, the $(pa)^2$ effects dominate and disagree with the completely off-shell improved result. Clearly we successfully confirm an independent

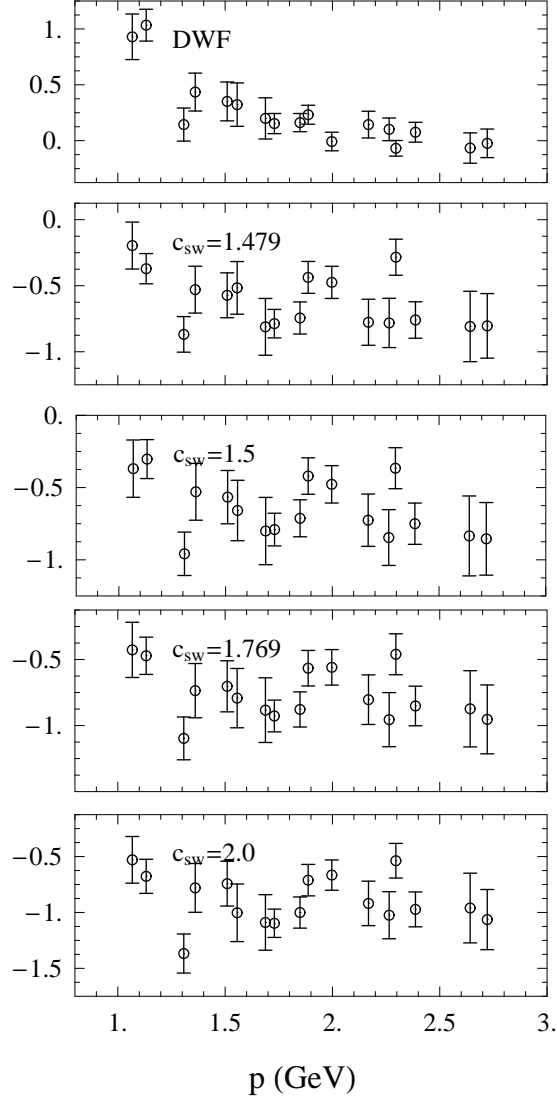


FIG. 12: The tensor vertex function form factor $\tau_5(p^2)/\overline{Z}_3(\overline{p})$ for the hard-recoil kinematics. This is displayed for both the chirally symmetric DWF action and the bare clover action.

method to determine c'_q .

VIII. DISCUSSION

We have calculated the form factors λ_1 , λ_2 , λ_3 , λ'_1 and τ_5 for both the bare clover action and the DWF action in two kinematic regions. We have numerically demonstrated rather clearly the automatic off-shell improvement of chiral fermion formulations.

Performing post-simulation rotations on the clover data can yield improved form factors. This involves worrisome systematic errors, such as the taking of $c_{\text{NGI}} = 0$, which are entirely avoided in the DWF formulation.

We demonstrate here that the use of the vertex function form factors as a means of fixing at least one im-

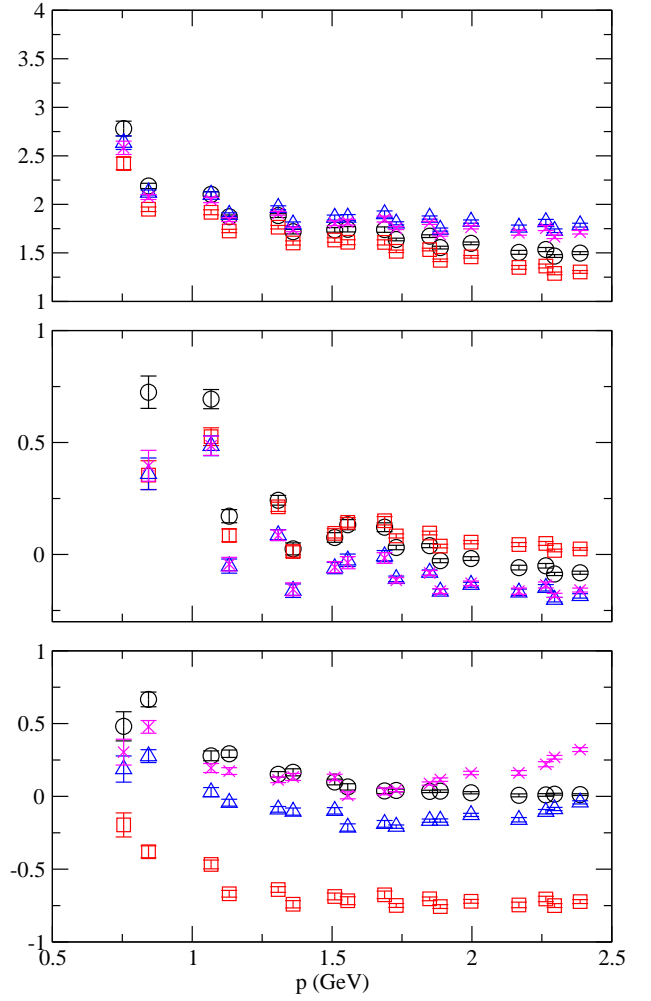


FIG. 13: The form factors λ_1 , λ_2 , λ_3 (from top to bottom) calculated with $q = 0$ kinematics and with various c'_q . The various actions are represented by different symbols: DWF (circles); NP clover with $c'_q = 0.0$ (squares), $c'_q = -0.20$ (triangles) and $c'_q = -0.257$ (crosses).

provement coefficient of the clover action in a manner that does not require the light quark limit. Unfortunately we have not been able to fix the crucial on-shell coefficient c_{SW} .

From the vertex form factors for the $q = 0$ kinematics, we showed that we can provide an independent way of determining the coefficient c'_q appearing in the improved quark field for the non-perturbatively improved clover action. Our finding of $c'_q = -0.257$ is very close to the tree-level prediction[10], -0.25 with the same tree-level b_q , or to the mean-field value of -0.285 with $b_q = 1.14$, and also to previous calculations[11] from the quark propagator alone.

We note that simulations with different clover coefficients and matched pseudoscalar masses produced identical vertex function form factors. One would naïvely expect to see a difference due to different choices of clover coefficient, particularly in the τ_5 form factor and

in the large momentum region where the leading perturbative behavior should dominate and the universal cut-off-insensitive infrared physics disappears. However, it seems that we have not yet reached a sufficiently fine lattice spacing where this perturbative intuition applies. Thus this coefficient cannot be fixed at these lattice spacings using this approach.

In contrast to the insensitivity to the clover coefficient, we see a large change in off-shell behavior between the entire clover class of actions and the domain wall action. In particular, since the domain wall action is $O(a)$ off-shell improved and this (un-rotated) clover action is not, large differences serve to demonstrate the effectiveness of the domain wall action, and it surely is a better action to study the vertex function in the future.

IX. SUMMARY AND OUTLOOK

We have studied the non-perturbative structure of two- and three-point functions for both the domain wall fermion action with an automatically $O(a)$ off-shell improved quark field, and for the on-shell improved clover action with various choices of the c_{SW} coefficient at fixed pseudoscalar mass. For the clover action the vertex function shows weak dependence on various choices of c_{SW} at

fixed pseudoscalar mass. Studying various Dirac structures at large momentum for the domain wall action showed vast improvements in the off-shell behavior of the theory. Also promising is the use of the behavior of the vertex function as a new method of fixing the $O(a)$ off-shell improved field coefficients for other fermion actions, in particular during the non-perturbative step scaling of relativistic heavy quark actions.

Comparison with the less-improved clover action allowed us to provide a new method to determine the coefficient c'_q through the form factor λ_3 . The result found was consistent with the value calculated from the quark propagator and previous published results. Further, this consistency may be taken as additional evidence that c_{NGI} is negligible.

ACKNOWLEDGMENTS

The author would like to thank RIKEN, Brookhaven National Laboratory and the U.S. Department of Energy for providing the facilities essential for the completion of this work and N. Christ, P. Boyle, C. Dawson, T. Izubuchi for useful discussions on various subjects and J. Skullerud for kindly providing both a vertex function calculation comparison and useful conversations.

-
- [1] M. Luscher, *et al.*, Nucl. Phys. B **491**, 323 (1997), hep-lat/9609035; M. Luscher, *et al.*, Nucl. Phys. B **491**, 344 (1997), hep-lat/9611015.
 - [2] A. X. El-Khadra, *et al.*, Phys. Rev. D **55**, 3933 (1999), hep-lat/9604004.
 - [3] J. E. Mandula, *et al.*, Phys. Lett. B **185**, 127 (1987); C. W. Bernard, *et al.*, Phys. Rev. D **49**, 1585 (1994), hep-lat/9307001; P. Marenzoni, *et al.*, Nucl. Phys. B **455**, 339 (1995), hep-lat/9410011; D. B. Leinweber, *et al.*, Phys. Rev. D **58**, 031501 (1998), hep-lat/9803015; D. Becirevic, *et al.*, Phys. Rev. D **60**, 094509 (1999), hep-ph/9903364; J. P. Ma, Mod. Phys. Lett. A **15**, 229 (2000), hep-lat/9903009; D. Becirevic, *et al.*, Phys. Rev. D **61**, 114508 (2000), hep-ph/9910204; H. Nakajima, *et al.*, Nucl. Phys. A **680**, 151 (2000), hep-lat/0004023; F. D. R. Bonnet, *et al.*, Phys. Rev. D **62**, 051501 (2000), hep-lat/0002020; F. D. R. Bonnet, *et al.*, Phys. Rev. D **64**, 034501 (2001), hep-lat/0101013; K. Langfeld, *et al.*, Nucl. Phys. B **621**, 131 (2002), hep-ph/0107141; P. O. Bowman, *et al.*, Phys. Rev. D **66**, 074505 (2002), hep-lat/020601.
 - [4] C. W. Bernard, *et al.*, Nucl. Phys. B (Proc. Suppl.) **17**, 593 (1990); C. W. Bernard, *et al.*, Nucl. Phys. B (Proc. Suppl.) **20**, 410 (1991); J. I. Skullerud, *et al.*, Phys. Rev. D **63**, 054508 (2001); J. I. Skullerud, *et al.*, Phys. Rev. D **64**, 074508 (2001); J. I. Skullerud, *et al.*, Nucl. Phys. B (Proc. Suppl.) **141**, 241 (2005); P. O. Bowman, *et al.*, Phys. Rev. D **66**, 014505 (2002); T. Blum, *et al.*, Phys. Rev. D **66**, 014504 (2002); F. D. R. Bonnet, *et al.*, Phys. Rev. D **65**, 114503 (2002); J. B. Zhang, *et al.*, Phys. Rev. D **70**, 034505 (2004); P. O. Bowman, *et al.*, Phys. Rev. D **70**, 034509 (2004), hep-lat/0402032.
 - [5] J. Skullerud, *et al.*, JHEP **0209**, 013 (2002), hep-ph/0205318; J. Skullerud, *et al.*, JHEP **0304**, 047 (2003), hep-ph/0303176; P. Boucaud, *et al.*, Phys. Lett. B **575**, 256 (2003), hep-lat/0307026; J. Skullerud, *et al.*, Nucl. Phys. B (Proc. Suppl.) **128**, 117 (2004).
 - [6] D. B. Kaplan, Phys. Lett. B **288**, 342 (1992), hep-lat/9206013; D. B. Kaplan, Phys. Proc. Suppl. **30**, 597 (1993); Y. Shamir, Nucl. Phys. B **406**, 90 (1993), hep-lat/9303005; V. Furman, *et al.*, Nucl. Phys. B **439**, 54 (1995), hep-lat/9405004.
 - [7] T. Blum, *et al.* (RBC), Phys. Rev. D **66**, 014504 (2002), hep-lat/0102005.
 - [8] H. Lin (2004), hep-lat/0409085.
 - [9] Sheikholeslami and R. Wohlert, Nucl. Phys. B **257**, 572 (1985).
 - [10] G. Martinelli, *et al.*, Nucl. Phys. B **611**, 311 (2001), hep-lat/0106003; D. Becirevic, *et al.*, Phys. Rev. D **61**, 114507 (2000), hep-lat/9909082.
 - [11] S. R. Sharpe, Nucl. Phys. B (Proc. Suppl.) **106**, 817 (2002), hep-lat/0110021; T. Bhattacharya, *et al.* Nucl. Phys. B (Proc. Suppl.) **106**, 786 (2002), hep-lat/0111002;
 - [12] Sheikholeslami and R. Wohlert, Nucl. Phys. B **257**, 572 (1985).
 - [13] T. Blum, *et al.*, Phys. Rev. D **69**, 074502 (2004), hep-lat/0007038.
 - [14] V. N. Gribov, Nucl. Phys. B **139**, 1 (1978).
 - [15] Y. Zhestkov, Ph.D. thesis (Columbia University), (2001).
 - [16] G. Martinelli, *et al.*, Nucl. Phys. B **445**, 81 (1995), hep-lat/9411010; V. Gimenez, *et al.*, Nucl. Phys. B **531**, 429 (1998), hep-lat/9806006; A. Doninir, *et al.*, Eur. Phys. J. C **10**, 121 (1999), hep-lat/9902030.

- [17] S. Mandelstam, Phys. Rev. D **20**, 3223(1979);
G. dell'Antonio, *et al.*, Nucl. Phys. B **326**, 333(1989).
- [18] D. B. Leinweber, *et al.*, Phys. Rev. D **60**, 094507 (1999),
hep-lat/9811027.